European Polymer Journal 240 (2025) 114320

Contents lists available at ScienceDirect

European Polymer Journal

journal homepage: www.elsevier.com/locate/europolj

Thermosensitive hydrogels based on Poly(VCL-co-VP) loaded with carbon nanotubes for cell culture: role of the functionalization on the neural cell growth

Pedro Liz-Basteiro [a,b,*], Goretti Arias-Ferreiro [c], Davide Marin [d], Enrique Martínez-Campos [a,e], Helmut Reinecke [a], Carlos Elvira [a], Juan Rodríguez-Hernández [a], Manuel Nieto-Diaz [f], David Reigada [f], Rodrigo M. Maza [f], Silvia Marchesan [d], Alberto Gallardo [a,**]

[a] Instituto de Ciencia y Tecnología de Polímeros (ICTP), CSIC, C/Juan de la Cierva 3, 28006 Madrid, Spain
[b] Departamento de Química Física, Universidad Complutense de Madrid, Avenida Complutense s/n, 28040 Madrid, Spain
[c] Center for Cooperative Research in Biomaterials (CIC biomaGUNE), Basque Research and Technology Alliance (BRTA), Paseo de Miramón 194, 20014 Donostia San Sebastián, Spain
[d] Department of Chemical and Pharmaceutical Sciences University of Trieste, Via L. Giorgieri 1, 34127 Trieste, Italy
[e] Grupo de Síntesis Orgánica y Bioevaluación, Instituto Pluridisciplinar (IP), UCM, Unidad Asociada al CSIC por el ICTP y el IQM, Paseo de Juan XXIII 1, 28040 Madrid, Spain
[f] Molecular Neuroprotection Group, Hospital Nacional de Parapléjicos (HNP), SESCAM, Finca La Peraleda s/n, 45071 Toledo, Spain

ARTICLE INFO

Keywords:
Thermosensitive hydrogel
Functionalized carbon nanotubes
Photopolymerization
Mechanical properties
Electrical conductivity
Cell manipulation
Cell sheet engineering

ABSTRACT

In this study, thermosensitive hydrogels based on vinyl-lactams, loaded with multi-walled carbon nanotubes (MWCNTs, hereinafter CNTs) in a range of weight percentages up to 0.3 %, have been prepared. To optimize charge dispersion in the polymeric network matrix, CNTs have been functionalized on the one hand to facilitate dispersion in the precursor formulation, and precursor formulations containing different percentages of two types of vinyl-lactams, vinylcaprolactam (VCL) and vinylpyrrolidone (VP), have been evaluated on the other. The incorporation of functionalized CNTs increased the compressive modulus of the hydrogels more than sixfold (from ~ 0.6 to ~ 3.7 MPa) and improved electrical conductivity by an order of magnitude (from $8.6{\cdot}10^{-3}$ to $8.1{\cdot}10^{-2}$ $S{\cdot}m^{-1}$), while promoting higher rates of adhesion and proliferation of endothelial and neuronal cells. These improvements highlight the potential of the developed system for biomedical applications, such as tissue engineering and regenerative medicine.

1. Introduction

Carbon nanotubes are among the most extensively studied nanomaterials, renowned for their excellent electrical conductivity and appropriate mechanical properties [1]. Liquid dispersions of carbon nanotubes are emerging functional advanced materials [2] that are seen as promising candidates for applications such as biocompatible transport, drug delivery, optical limiting, optical sensors, etc. [3–5]. In addition, research has shown that the modification of materials such as hydrogels with carbon nanotubes can significantly enhance their specific biofunctions [6], making them highly attractive for applications in tissue engineering. In this work, we specifically address the multi-walled carbon nanotubes (MWCNTs, hereinafter CNTs) loading of thermosensitive hydrogels based on the vinyl-lactam *N*-vinylcaprolactam (VCL). These hydrogels, with a volume phase transition temperature, VPTT, close to 34 °C, have shown their capacity to serve as cell culture supports at 37 °C, and to allow a non-aggressive cell detachment, even of entire cell monolayers, by a simple temperature decrease [7–10]. Thus, loading a hydrogel with CNTs may be of interest to improve properties such as mechanical or electrical and ultimately also influence cell response.

Loading hydrogels, hydrophilic networks swollen in water, with

* Corresponding author at: Instituto de Ciencia y Tecnología de Polímeros (ICTP), CSIC, C/Juan de la Cierva 3, 28006 Madrid, Spain.
** Corresponding author.
E-mail addresses: pedroliz@ictp.csic.es (P. Liz-Basteiro), gallardo@ictp.csic.es (A. Gallardo).

https://doi.org/10.1016/j.eurpolymj.2025.114320
Received 17 July 2025; Received in revised form 23 September 2025; Accepted 25 September 2025
Available online 9 October 2025

CNTs, remains a significant challenge because CNTs exhibit poor dispersibility in aqueous medium and poor compatibility with hydrophilic structures (or highly hydrophilic ones in the case of ionic hydrogels). Nevertheless, in spite of this challenge, CNTs nanocomposite hydrogels have demonstrated remarkable improvements compared to conventional hydrogels in mechanical properties and toughness [11], electrical conductivity [12], thermal stability [13] and rapid sensor response [14]. Indeed, the applications of CNTs nanocomposite hydrogels span various fields of human endeavor such as sensoring, solar cells or biomedicine [15]. Carbon nanotubes (CNTs) improve cell adhesion by mimicking the extracellular matrix (ECM) at the nanoscale, interacting favorably with cell adhesion proteins and receptors [16]. In addition, their electrical conductivity can also benefit the growth of certain cell types, such as osteoblasts [17].

Thermosensitive polymeric chains in aqueous media, such as those derived from VCL, are non-ionic and base their thermosensitivity on an appropriate amphiphilicity. Importantly, amphiphilic polymers have been found to be good dispersing agents for CNTs [18–20]. Therefore, in this work we hypothesize that CNTs can be loaded on thermosensitive hydrogels through a two-step procedure, *i.e.* dispersion of CNTs in the VCL-based amphiphilic formulation, followed by a mass polymerization step. Since VCL is solid at room temperature, in this work the use of another vinyl lactam, *N*-vinylpyrrolidone (VP), structurally related to VCL, is proposed as a comonomer/dispersing agent. In the context of CNT dispersion, it is well known that polyVP, in addition to being highly cytocompatible [21], is an excellent non-ionic polymeric surfactant [22] and, although amphiphilic, it is slightly more hydrophilic than VCL. As a result, the use of VP therefore allows a simplified, solvent-free dispersion design, using only the polymerizable components (hydrogel chain units after polymerization), and avoiding water and/or solvents that can have a negative effect on the dispersion.

Since the hydrogel will consist of crosslinked poly(VCL-co-VP) chains, we first investigated how the incorporation of VP affects the thermosensitivity of VCL-based hydrogels, as well as other properties such as the cell response. To this end, hydrogels with different molar ratios of VCL/VP were prepared, characterized, and evaluated. After this initial study, the most appropriate system was selected to disperse the CNTs and prepare the nanocomposites. This optimized system was evaluated using adherent endothelial and neural cell lines in order to analyse biological processes such as adhesion, proliferation, and transplant ability [23]. In addition, the conductivity properties of the hydrogel can improve cell-to-cell and cell-to-scaffold communication, and coupled with electrical stimulation, may enable the transmission of electrical signals to electroactive tissues such as the central nervous system [24,25].

The novelty of this work lies in a two-step strategy: 1) dispersion in a solvent-free photocurable formulation, followed by 2) photopolymerization. VP acts simultaneously as a comonomer and dispersing agent. Furthermore, since CNTs are functionalized with polymerizable groups, an improved integration into the polymer matrix is expected. In short, our hypothesis is that this preparative design can improve the dispersion of CNTs within the poly(VCL-co-VP) matrix, which may lead to improved hydrogel properties and influence cell response.

2. Experimental section

2.1. Materials

N-vinyl caprolactam (VCL), ethylene glycol dimethacrylate (EGDMA), 1-hydroxyl cyclohexyl phenyl ketone (HCPK), 4-vinylaniline (VA), isoamyl nitrite (IAN), *N*-dimethylformamide (DMF), acetonitrile (MeCN), methanol, and diethyl ether were supplied by Sigma-Aldrich (St. Louis, MO, USA). 1, 3-divylimidazolidin-2-one (DVI) was supplied by BASF. *N*-vinylpyrrolidone (VP) was supplied by Acros Organics. Multi-wall carbon nanotubes (CNTs) were purchased from Elicarb (diameter: 15–20 nm). Reagents and solvents were used as supplied, unless indicated differently.

Autofluorescent C166-GFP endothelial murine cell line expressing green fluorescent protein (GFP), was purchased by ATTC-(CRL-2583; RRID#CVCL 6582). Fetal bovine serum (FBS) was purchased from Thermo Scientific (Hyclone®, Thermo Scientific, Waltham, MA, USA). Phosphate buffered saline (PBS), Dulbecco's Modified Eagle Medium (DMEM), the antibiotic (penicillin, streptomycin (P/S), and G418), and glutaMAX were also supplied by Sigma-Aldrich. 12 and 24 well culture plates (treated and untreated, respectively) were purchased from Corning Costar (New York, NY, USA). For neural cultures, Neuro2a mouse neuroblastoma cell line (cat# CCL-131, ATCC; RRID#CVCL_0470) was purchased from ATTC. 48 and 96 wells culture plates were purchased from Thermo Scientific (Rochester, NY, USA).

2.2. Functionalization of CNTs

CNT functionalization was performed in DMF and MeCN. First, 15 mg of CNTs were placed in 15 mL of DMF sonicated for 30 min at room temperature (20 °C, RT). Next, the proper amount of 4-vinylaniline and isoamyl nitrite were added in 15 mL MeCN (see Table 2) to the previous mixture and then refluxed for the selected time at 80 °C and 200 rpm.

The mixture was filtered with a Millipore membrane (JHWP, 0.45 μm) and washes were performed with 2x DMF, 1x MeCN, 1x water, 1x MeOH, 1x DMF, 1x MeCN, 1x water, 1x MeOH, 2x diethyl ether. The following day the powder was dried in an oven (80 °C) for 6 h.

2.3. Synthesis of the hydrogels by photopolymerization

Thermosensitive hydrogels were prepared from the polymerizable precursors by conventional radical photopolymerization [26] in one single step. Different VCL/VP molar ratios were evaluated, between 100/0 and 0/100 as shown in Table 1. The crosslinkers added were DVI and EGDMA in molar percentages of 0.574 and 1.066, respectively, against the total monomer content. HCPK was used as a photoinitiator at 0.5 % weight.

In the case of the hydrogels loaded with CNTs, formulations with different weight percentages of CNTs were prepared (see Table 3; 0 wt% was prepared as control). The photopolymerizable mixtures were stirred for 5 min. Subsequently, CNTs were added and the mixtures were stirred again for 5 min, followed by sonication for 30 min.

All the mixtures were injected into molds and photopolymerized in a curing chamber. The molds were prepared from polystyrene sheets covered with polyethylene film and separated both by commercial silicone with a thickness of 0.3 mm. The photopolymerization was carried out inside a UV chamber that generate close to 3500 $\mu W/cm^2$ (model CL-1000l, 230 V), for 40 min and $\lambda = 365$ nm. After obtaining the hydrogels, the hydrogel mold was removed, and successive washes were performed with distilled-H_2O to remove any residual mixture and achieve equilibrium between the hydrogel and the medium.

2.4. Materials for characterization methods

Transmission electron microscopy (TEM) was carried out on a JEM 2100 (Jeol, Tokyo, Japan) at 100 kV. Samples were dispersed in DMF via ultrasonic treatment to obtain a light grey dispersion, then 2 μL of the samples were dropcasted onto TEM carbon grids previously exposed to a UV-Ozone Procleaner Plus for 5 min and dried in vacuo.

Thermal analyses were carried out in a thermogravimetric analyzer (TGA) controlled by METTLER instrument. 1–2 mg of powdered sample was heated from 0 up to 800 °C, by equilibrating at 100 °C for 20 min. The experiments were performed under nitrogen flow, using a slow temperature increment (10 °C/min).

Raman spectra were acquired on five different spots per sample with an InVia 50 Renishaw Raman Microscope equipped with laser at 532 nm (25 mW), with 10 accumulations, 1 cm^{-1} resolution. Samples were prepared on microscopy glass slides and at least 5 replicas.

2.5. Hydrogels characterization methods

Transmittance values of hydrogels were determined in a UV–Vis SPECORD 205 spectrophotometer associated with the WinASPECT software, which was used at a visible wavelength (600 nm) in PBS at 37 °C by triplicate. The hydrogels were stabilized in the medium 24 h before the test to ensure a complete polymer-medium equilibrium.

Swelling tests of the photopolymerized hydrogels were performed in Phosphate Buffered Saline (PBS) solution (pH = 7.4). Hydrated hydrogels were die-cut into 7 mm diameter cylinders prior to testing. After that, the hydrogels were immersed in 15 mL of PBS at different temperatures (ranging from 5 to 80 °C). The pieces were weighted at different times to follow the swelling process. All the samples were measured by triplicate. The swelling percentage (S) was determined from Eq. (1):

$$S = \frac{(w_S - w_D)}{w_D} \cdot 100 \quad (1)$$

where w_S and w_D are the weights of the swollen and dry systems, respectively.

The mechanical properties of the hydrogels were analysed based on dynamic compression tests. Measurements were performed on hydrogels hydrated at 20 °C immersed in distilled water, using a universal test system (MTS System, ® QTest1/L Elite) in compression mode. Cylindrical samples with a diameter of 7 mm and thickness of around 0.5–0.7 mm were used (hydrogels were die-cut prior to the assay at 20 °C to ensure correct dimensions). Samples were placed between compression platens, with the upper one being 5 mm of diameter. Each sample was subsequently deformed to a specific compressive strain level at 0.5 mm/min. All measurements were performed in quintuplicate and analysed with a 100 N Charge Cell associated with TestWorks software.

Oscillatory rheological characterization was carried out using a strain-controlled rheometer (Malvern Kinexus Ultra Plus Rheometer) with a parallel-plate geometry (20 mm diameter) at a fixed temperature of 20 °C using a Peltier temperature controller. The hydrogels were measured at a shear rate between 0.1 and 100 s^{-1}. Frequency sweeps recorded at 2 Pa from 0.01 to 10 Hz. Stress sweeps were performed from 1 Pa up to hydrogel failure at 1 Hz. For every type of hydrogel, three measurements were performed to confirm the reproducibility of the measurements.

Electrical conductivity (σ) at room temperature was calculated using a conventional four-point probe method (Ossila, Sheffield, United Kingdom) with a target current set in the range between 10 and 100 μA using 10 V as the maximum voltage. The hydrogels were cut into circles with a diameter of 10 mm and kept in water until they were measured. The final thickness (t) of the wet samples was then measured with a caliper before the measurement. Electrical conductivities (σ) reported for each polymer formulation are averages of at least three different samples.

The surface wettability of the hydrogels was measured at room temperature by the capillary rise technique [27]. A 0.3 cm × 2 cm hydrogel piece was placed vertical to an aqueous solution. When the hydrogel contacts the surface of the water a capillary quickly rises along the vertical hydrogel. According to the literature, the height of the meniscus is an indirect measurement of the hydrophilicity of a plate, in this case, the hydrogel [28].

2.6. Biological evaluation of thermosensitive networks

2.6.1. Cell studies protocol

Hydrogels with a diameter of 10 mm, tailored to fit into a 12-well plate, were die-cut in distilled water at 37° C. Subsequently, for the hydrogels were sterilized following this procedure. The networks were first washed through three times with 70 % ethanol for 10 min each. Following this step, the hydrogels underwent extensive washing three times with PBS at pH 7.4. The samples were then irradiated with UV light for 20 min on each side. Following the UV treatment, a final wash with high-glucose Dulbecco's Modified Eagle Medium (DMEM; D6429) was performed. The samples were then immersed in complete DMEM containing 1 % P/S (100 U/mL penicillin) and 10 % FBS and incubated overnight in a cell incubator at 37 °C and 5 % CO_2.

C166-GFP cell line with the GFP gene integrated that ensures constitutive expression and inherent autofluorescence that enables real-time monitoring via fluorescence microscopy, was utilized as a cytocompatibility model. Cells were seeded onto the hydrogels at a density of $2x10^4$ cells/cm^2 in 12 well plates and cultured in high-glucose complete DMEM in a cell culture incubator at 37 °C in a humidified atmosphere containing 5 % CO_2. Passage of cells occurred upon reaching approximately 90 % confluence.

2.6.2. Quantitative analysis of cell adhesion by optical microscopy

Focal adhesion of the cells was studied through image analysis by monitoring the surface of the hydrogels at two different times 4 and 24 h after cell seeding. Samples were imaged in triplicate for quadrant analysis with ImageJ software taking five quadrant images with resolution of (x, y) = (750, 550) μm. Cells were labeled as adhered (stretched) or not adhered (rounded) according to the displayed morphology.

2.6.3. Cell sheet detachment using a controlled temperature decrease

After 48 h of cell culture proliferation, the cultures were transferred to new tissue culture plates using a controlled temperature decrease method. First, fresh culture medium was added to the new plate, comprising 70 % of the total volume to maintain moisture on the contact surface. Subsequently, the hydrogels were inverted and placed onto the new plate, allowing the cell culture to contact the surface of the well plate. The remaining 30 % of culture medium was then added. This process ensured that the samples were maintained at 15–20 °C for 40 min. Finally, the hydrogels were removed, and the plates containing the cell transplants were reincubated at 37 °C and 5 % CO_2.

2.6.4. Cell proliferation study, quantify dsDNA. Fluorimetry assay

The quantification of double stranded DNA content of the samples was analyzed, 48 h after seeding stage using the FluoReporter® Blue Fluorometric dsDNA Quantitation Kit (F-2962). The analysis was developed in accordance with the kit instructions. Briefly, the samples were frozen overnight at −80 °C. Subsequently, they were thawed at RT and then covered with 300 μl of distilled water to ensure complete coverage of the hydrogel layer with proliferating cells. The plates were then incubated at 37 °C for 1 h, followed by a 20 min freezing period and subsequent thawing at RT. For quantitative analysis, an additional 300 μL of Hoechst 33,258 reagent mixed with the kit's TNE buffer in a 1:4 ratio was added. DNA content analysis was performed in triplicate using a plate reader (Synergy HT, Brotek) with excitation/emission wavelengths set at 346/460 nm.

2.6.5. Metabolic activity. Alamar Blue

Metabolic activity was analyzed using Alamar Blue assay (Biosource, CA, USA), in accordance with the manufacturer's instructions. This method, recognized for its non-toxic nature and scalability, quantifies the cellular reducing power, primarily reflective of mitochondrial activity, thereby providing an approximation of cell viability and cytotoxicity. The study was carried out in triplicate, with 10 % of the staining reagent added to the total volume, followed by a 90 min incubation period. Fluorescence measurements (λex/λem 535/590 nm) were performed in three independent experiments using a plate reader.

2.7. Neural cell culture evaluation

2.7.1. Neural cell culture

To evaluate the hydrogel neurotoxicity and their effects on neural

cells, we used the Neuro2a mouse neuroblastoma cell line. In a basal state, Neuro2a cells display two main morphologies when cultured on plastic in standard 10 % serum medium: an amoeboid phenotype, characterized by weak substrate adhesion and a rounded shape that favours rapid proliferation; and a neuronal stem cell-like phenotype, characterized by a flatter shape with non-functional neurite extensions and stronger adhesion mediated by extracellular proteins such as integrins. These "neuronal stem cell" characteristics does not signify the initiation of a differentiation process, which requires an inductive signal to be actively triggered. Neuro-2a cells were cultured in DMEM supplemented with 10 % FBS, 1 % P/S, and 1 % glutaMAX at 37 °C in a humidified incubator containing 5 % CO_2. After 3 to 5 passages, cells were seeded on 96 or 48 well plates bearing the hydrogels washed and sterilized as described in 2.7.1.

2.7.2. Cell viability assay

The effect of hydrogels on Neuro2a viability was measured via the (4,5- dimethylthiazol-2-yl)-2,5-diphenyltetrazolium bromide (MTT) assay. Briefly, around 10,000 Neuro-2a cells per well were seeded on top of the hydrogels in 96-well plates in a 10–20 μL drop, left for 10 min to adhere to the hydrogel, and then 100 μL of the culture medium was added. After 48 h, the hydrogel and the culture well were separately incubated with 0.5 mg/mL of MTT reagent (Sigma-Aldrich) for 1 h at 37 °C and solubilized with 100 μL of hydrochloric acid 0.1 M diluted in isopropanol for 20 min shaking at RT. Finally, absorbances at 570 and 660 nm were determined using a plate reader luminometer (Infinite M200, Tecan Group LTD. Mannendorf, Switzerland). Analyses were replicated in two independent experiments.

2.7.3. Video time lapse analysis of morphology, proliferation and migration

Around 20,000 Neuro2a cells per well were seeded on top of the hydrogel in 48 wells culture plates, followed by the addition of the culture medium. After allowing them to adhere for 4 h, they were taken to a Leica DMI6000B automatic inverted microscope prepared for Video Time Lapse (temperature and humidity maintenance, motorized stage) and equipped with a Leica DFC 350 FX ultra-high sensitivity monochrome digital camera. The system was scheduled to capture images every 20 min for 48 h at 5 positions in each well. As a result, 725 images were taken for each hydrogel–bearing well using a 20X objective (HCX PL FLUOTAR 20x/0.40 CORR PH). One additional well without hydrogels was also seeded and imaged as a control. The resulting images were analyzed using FIJI 2.14.0 software (Schindelin *et al.*, 2012), following the evolution of selected cell clusters over 48 h and assessing their morphology throughout the process.

3. Results and discussion

3.1. Influence of VP on the properties of unloaded hydrogels

This work addresses the preparation of nanocomposite hydrogels, *i.e.*, thermosensitive hydrogels based on VCL loaded with CNTs. Firstly, the CNT used as fillers were dispersed in the monomeric precursors' mixture (*i.e.,* VCL + VP), followed by light curing. In order to use an appropriate VCL/VP mixture, we first studied the influence of VP addition on the properties of the unloaded hydrogels.

This study has been carried out using a previously described formulation, which yielded robust VCL-based hydrogels with excellent performance in cell manipulation [8,10]. Specifically, a mixture of crosslinkers (see experimental section) was used at a molar percentage of 1.61 mol % with respect to vinyl-lactams. Samples were prepared with different VCL/VP molar ratios, and labeled as HYDX being X the VP molar %, as shown in Table 1. In all cases, crosslinked films were obtained.

VP, as previously mentioned, is a hydrophilic monomer, so an increase in swelling is to be expected as the VP content increases, as well as a shift of the VPTT towards higher temperatures, as it has been described for copolymers of *N*-isopropyl acrylamide, NIPAAm, and hydrophilic monomers [29].

Fig. 1 illustrates the gradual swelling variations as a function of temperature (10–80 °C) for hydrogels with different compositions (ranging from 0 to 100 mol% of VP content). All the hydrogels, independently of the composition, presented a larger swelling at lower temperatures and decreased upon heating. However, as it can be observed, the swelling variations between low and high temperatures, as well as the temperature range of the swelling transition with temperature, largely depend on the VP content. VCL-based thermosensitive hydrogels are characterized by showing, when heated from temperatures below the VPTT, an abrupt decrease in swelling until reaching a plateau of low water content once the VPTT is exceeded.. This behavior can be easily observed in hydrogels with VP contents up to 50 wt% (HYD50), for which it has been possible to determine VPTT values (calculated as indicated in the experimental section). VPTT increases with the presence of a hydrophilic unit as VP. However, hydrogels with VP contents of 70 wt% (HYD70) or higher did not appear to have reached this plateau yet, *i.e.*, we can hypothesize that the VPTT values can be found at either unmeasured or unobservable temperatures (if possible, above 100 °C). In any case, the latter hydrogels have been discarded for the rest of the study.

Regarding the swelling values of HYD50 and hydrogels with lower VP content, a general trend is observed, showing that the change in absorbed volume increases with the molar percentage of VP. This indicates that a higher VP content leads to greater sensitivity to temperature changes, affecting the swelling behavior of the hydrogels. Table 1 lists swelling values for three representative temperatures, including 37 °C. Hydrogels with VP content of 30 % (HYD30) and below are found in, or close to, a less hydrophilic region, indicating a lower affinity for water at this temperature. Conversely, as the VP content reaches 50 % (HYD50), the hydrogels shift to more hydrophilic regions, demonstrating a greater water affinity. This change in hydrophilicity directly affects the hydrogel properties and its interactions in aqueous environments, which are crucial for applications involving cell culture and other biomedical uses.

VCL-based hydrogels have been previously described as robust and easy to handle, and have shown moduli at RT in the range of 0.1–1 MPa[7]. In this work, the influence of VP content on the mechanical properties has been evaluated at RT, *i.e.* below the VPTT, by swelling compression measurements (see experimental section). The modulus and other parameters are listed in Table 1. Although all hydrogels (HYD0 to HYD50) have been shown to be easy to handle, increasing the VP content has resulted in a decrease of the modulus, which has been evidenced to be dependent on the hydrogel composition. This decrease is correlated with the increase in water content, *i.e.*, the higher is the water content, the lower will be the modulus. The moduli values decrease from about 1.3 MPa in the HYD0 hydrogel at 20 °C (a value in the range of standard hydrogels) [30], to values of approximately 500 KPa for hydrogels with VP content of 50 mol % (HYD50) measured at the same temperature.

In order to first validate the use of these hydrogels (*i.e.*, HYD0 to HYD50) for biological applications, their cytocompatibility was assessed, as well as their ability to enable non-aggressive cell detachment by lowering the temperature. To this end, VCL-based hydrogels were seeded with an endothelial murine cell model and cell monolayers proliferated over their surface, demonstrating their cytocompatibility (see Fig. 2a). Moreover, cell cultures were adequately transplanted to a new plate by temperature decrease, showing a high cell detachment efficiency. Table 1 and Fig. 2b shows the cell metabolic activities after 24 h of transplantation.

3.2. Preparation of the hydrogel composites with CNTs: Dispersion and loading of the CNTs

As mentioned in the introduction, the hydrogel loading procedure is based on an initial dispersion of CNTs in the VCL/VP precursor mixture

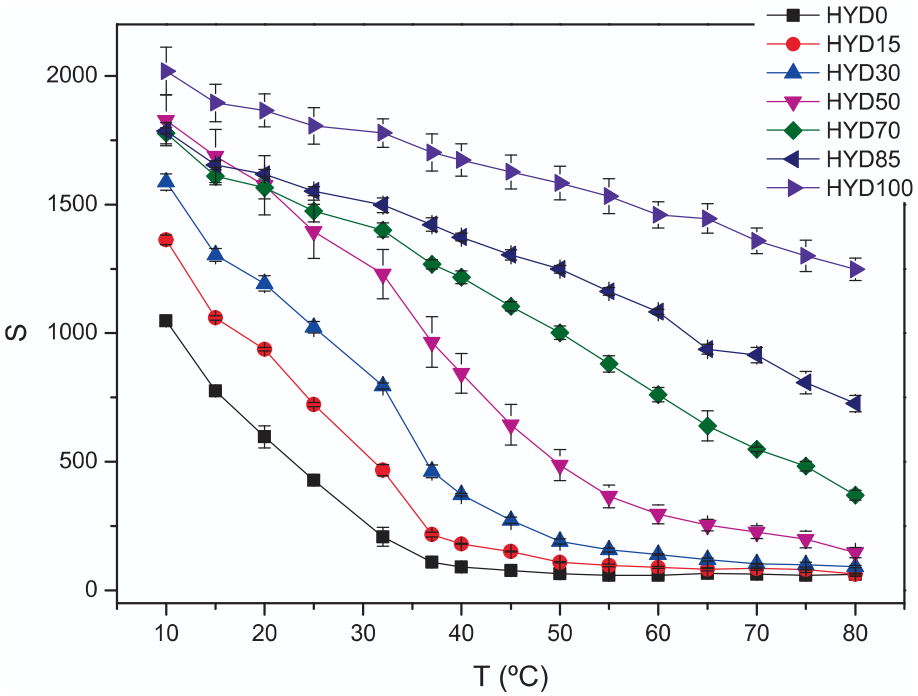

Fig. 1. S, swelling percentage in PBS (determined as indicated in 2.5 and Eq. (1), as a function of temperature, T, of the hydrogels prepared using variable VCL/VP ratios (100/0, 85/15, 70/30, 50/50, 30/70, 15/85 and 0/100).

Table 1
Swelling percentage (S), VPTT, mechanical properties values and data from the fluoreporters dsDNA assay on the hydrogels after 48 h of the seeding process, of the different unloaded VCL-VP hydrogels.

Label	VP/VCL molar ratio	S at (°C)			VPTT (°C)	Maximum Load (N)	Elongation (%)	Elastic Modulus (MPa)	Fluorescence Intensity (A.U.)
		10	37	60					
HYD0	0/100	1050 ± 20	110 ± 10	59 ± 3	32	19 ± 1	77 ± 1	1.3 ± 0.2	926 ± 27
HYD15	15/85	1360 ± 20	217 ± 9	90 ± 4	39	13 ± 2	79 ± 2	0.8 ± 0.2	922 ± 35
HYD30	30/70	1590 ± 30	463 ± 25	140 ± 3	46	12 ± 1	82 ± 2	0.6 ± 0.2	896 ± 18
HYD50	50/50	1830 ± 100	965 ± 98	296 ± 37	52	10 ± 2	88 ± 6	0.5 ± 0.2	899 ± 22
HYD70	70/30	1780 ± 40	1270 ± 20	761 ± 28	–	–	–	–	–
HYD85	85/15	1790 ± 10	1420 ± 30	1080 ± 10	–	–	–	–	–
HYD100	100/0	2020 ± 90	1700 ± 70	1460 ± 50	–	–	–	–	–

(without additional solvent). As expected, pristine CNTs did not display an acceptable dispersibility [31–33]. Therefore, initial efforts focused on the CNT functionalization to improve their dispersibility. To this end, CNTs were treated with 4-vinylaniline and nitrite to perform the widely known Tour reaction (Scheme 1) [31,34–37]. It should be noted that this functionalization provides potentially polymerizable styrenic groups.

3.2.1. *CNT functionalization*

Based on previous works [31], the harsh conditions listed in entry 1 of Table 2 were initially tested. TGA was used to determine the functionalization degree (as wt. %); this calculation is based on the weight loss of treated CNTs at 600 °C compared to pristine CNTs at the same temperature [38]. These conditions resulted in a functionalization of around 15 wt% (see Fig. 3a), which is relatively high (it has been labeled as HF-CNT, with HF indicating high functionalization). However, this functionalizing to a large extent is related to a consistent number of defects in the CNT structure, thus negatively affecting their final electronic properties [39]. Therefore, the milder conditions of entries 2 and 3 were selected and explored, which resulted in wt. % functionalization corresponding to 11.6 and 4.2 wt%, respectively. These samples have been correspondingly labeled as MF-CNT (medium functionalization) and LF-CNT (low functionalization). Therefore, the functionalization degree can be modulated by varying the reagent concentrations and the reaction time. A complete description of the three procedures can be found in the Experimental Section.

Pristine, HF-CNT, MF-CNT, and LF-CNT samples have also been characterized by Raman spectroscopy, as shown in Fig. 3b. The characteristic peaks corresponding to the G and D bands appear at 1590 cm^{-1} and 1350 cm^{-1} respectively [40–42]. The D band is related to the sp^3 states of carbon, and it is used as an indication of the level of disruption of the aromatic p-electrons system on the nanotube sidewalls [43]. The ratio of the intensities of the Raman signals associated with disordered and ordered transitions (I_D/I_G) gives valuable information regarding the effectiveness of the functionalization. The I_D/I_G value

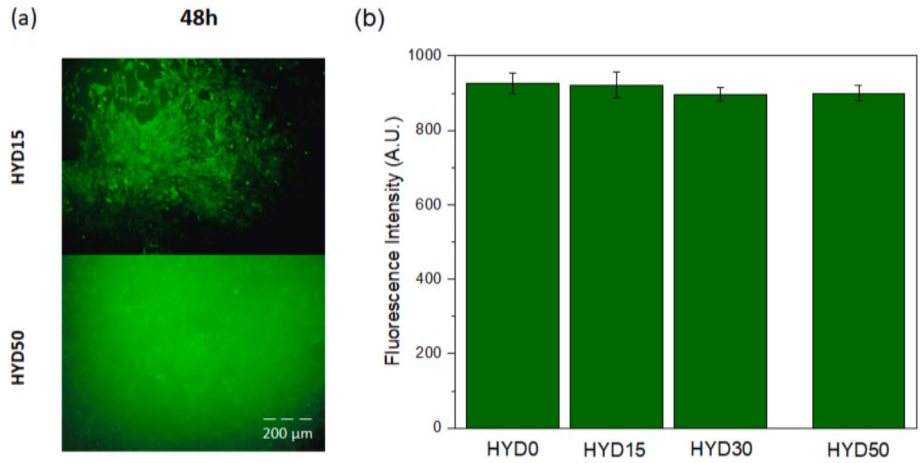

Fig. 2. (a) Fluorescence images of C166-GFP cell cultures on the HYD15 and HYD50 hydrogels 48 h after seeding process (scale bar: 200 µm). (b) Alamar Blue assay on the cell transplants from the hydrogels after 24 h of the transplantation process.

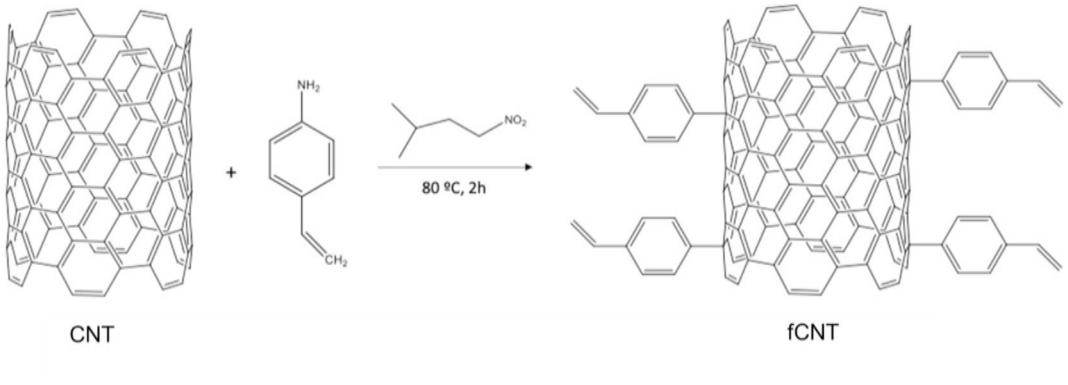

Scheme 1. Tour reaction on CNTs with 4-vinylaniline and isoamyl nitrite.

Table 2
Functionalization reaction conditions and characterization by Raman spectroscopy and TGA. Representative TEM images are shown at the top.

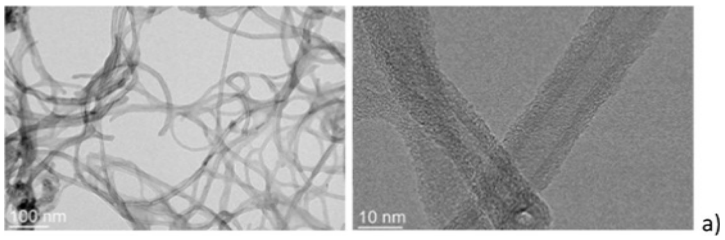

	VA/IAN/CNTs (µL/µL/mg) [b]	Reaction Time (h)	CNT functionalization (wt.%)	CNT functionalization (styrenic moiety mmol/g CNT)	(I_D/I_G)[c], Raman
1. HF-CNT	180/300/15	2.0	14.2 ± 1.1	1.4 ± 0.1	1.10
2. MF-CNT	110/250/15	1.5	11.6 ± 0.6	1.1 ± 0.1	1.13
3. LF-CNT	44/200/15	1.0	4.2 ± 0.2	0.4 ± 0.0	1.37
pristine CNT	n.d.	n.d.	0	0	1.52

a) TEM images of the HF-CNT after dispersion in DMF and drying (scales 100 and 10 nm).
b) VA = 4-vinylaniline: IAN = isoamyl nitrite.
c) Ratio of Raman intensities of the D and G bands of CNTs (I_D/I_G) from Raman spectra.

varies from 1.52 for pristine CNTs to 1.37 in functionalized LF-CNT, 1.13 in MF-CNT, and 1.10 in HF-CNT. The observed trend is the result of the attachment of styrene functional groups onto the CNTs, which is composed solely of sp^2 carbon atoms that are characterized by an intense Raman signal at ~ 1585 cm^{-1}, thus overlapping with the D band. As the functionalization level increases, the styrene aromatic signal at 1180 cm^{-1} becomes visible in MF-CNTs and HF-CNTs [44]. Furthermore, MF-CNTs and HF-CNTs spectra displayed additional signals in the range between 1608 and 1626 cm-1 that could be ascribed to 4-vinyl aniline, thus suggesting an additional level of non-covalent functionalization, which can be beneficial for further improvement in homogeneity of nanocomposites with CNTs [45].

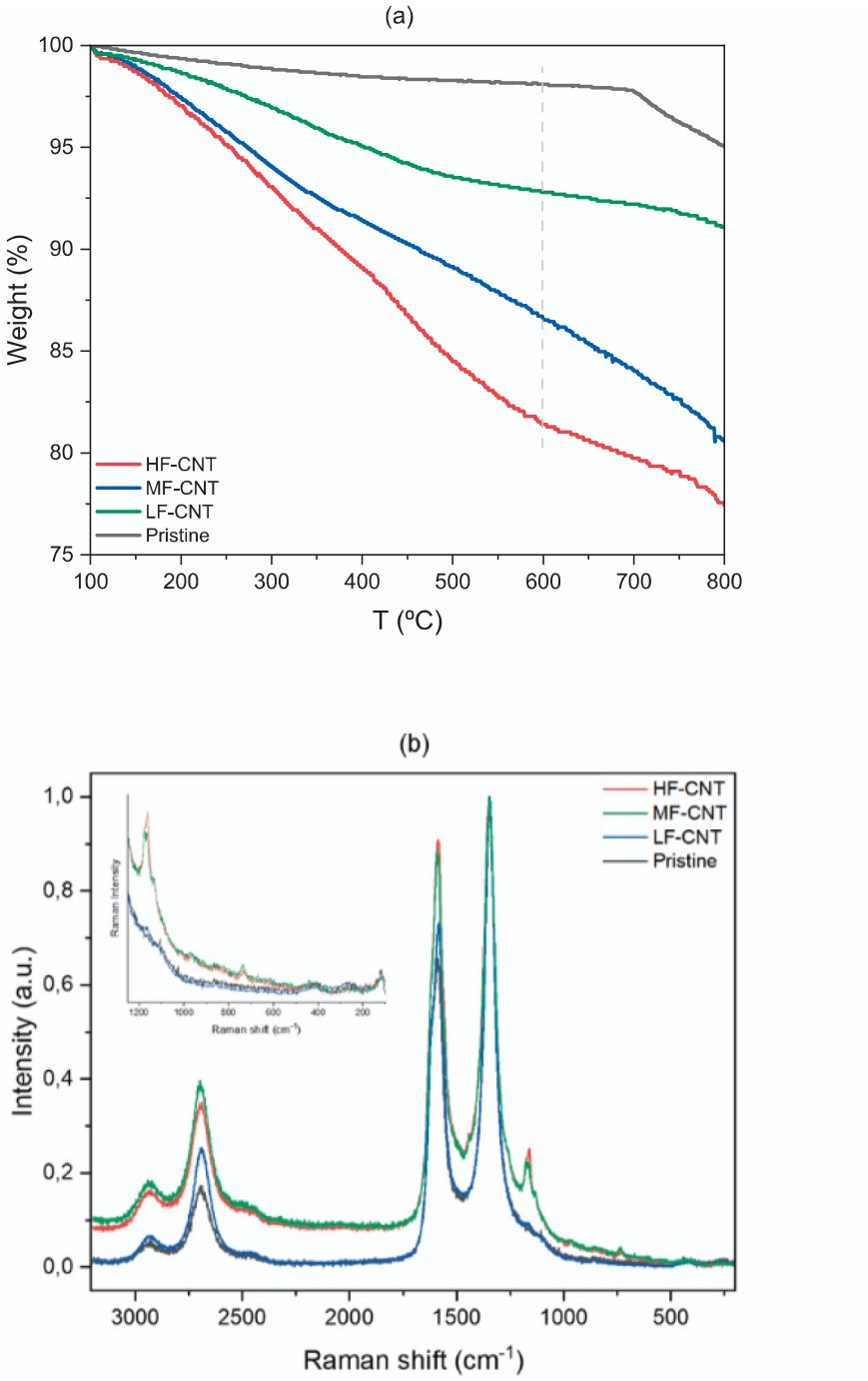

Fig. 3. (a) Thermograms of the CNTs: pristine, LF-CNT, MF-CNT and HF-CNT. The dashed line marks the temperature of 600 °C that was used to calculate the functionalized level. (b) Raman spectra (532 nm excitation) of pristine CNTs and CNTs with different degrees of functionalization (*i.e.*, LF-CNT, MF-CNT, and HF-CNT).

3.2.2. CNT dispersion and photocuring

Based on the previous study in section 3.1, HYD15 and HYD30 have been selected as candidates for CNTs dispersion and preparation of loaded hydrogels after photocuring as the VPTT should be kept as close to 37 °C as possible. The CNTs functionalized according to the previous section dispersed much better than the pristine CNTs in the VCL/VP 85/15 and 70/30 photocurable formulations. It is worth noting that CNTs dispersed faster in the VCL/VP 70/30 mixture than in the 85/15, so the former was the one selected for the rest of the study. This is probably due to the higher content of VP, a known surfactant unit. Therefore, we focus our analysis on the HYD30 loaded with the different functionalized CNTs.

Table 3 provides the general picture of the dispersibility of functionalized CNTs (*i.e.*, HF-CNT, MF-CNT, and LF-CNT) in a 70/30 (molar ratio) VCL/VP-based formulation. In particular, four weight percentages were assessed, *i.e.*, 0.01, 0.1, 0.3, and 0.5 wt%. As expected, the CNTs with the highest functionalization level (*i.e.* HF-CNT) were the most easily dispersed up to a weight percentage of 0.3%, which was the highest wt % used. Nevertheless, also the other CNT samples (*i.e.*, LF-CNT and MF-CNT) could be dispersed, but only at loading as low as

Table 3
The dispersibility of the different CNTs at several wt.% is shown.

Wt.% CNTs In VCL/VP	Pristine	LF-CNT	MF-CNT	HF-CNT
	Dispersion in VCL/VP 70/30 mixture*			
0.01	LOW	HIGH	HIGH	HIGH
0.1	LOW	MEDIUM	MEDIUM	HIGH
0.3	LOW	LOW	LOW	HIGH
0.5	LOW	LOW	LOW	LOW

* It is considered a LOW dispersion when the photocurable formulation was not a homogeneous liquid dispersion. A dispersion was considered MEDIUM when it could be photocured but the resulting hydrogel was macroscopically heterogeneous (agglomerates were perceived even to the touch). A HIGH dispersion was when a macroscopically homogeneous hydrogel could be obtained after light curing.

0.01 wt%.

Pristine CNTs did not disperse at any of the concentrations tested, which is not surprising considering their high tendency to aggregate. Based on these results, HF-CNT were chosen for the preparation of hydrogels HYD30 with different CNT content, even though a higher number of defects in the CNTs structure is to be expected with such a high functionalization level [46]. On the other hand, as mentioned above, the styrene groups resulting from the functionalization are potentially polymerizable, so it is expected that they will participate in the photocuring reaction, leading to stable covalent integration of the CNTs. Related strategies to achieve good dispersion of CNTs [47] have recently been described.

Hydrogels listed in Table 4 were prepared by photocuring a formulation containing VCL/VP in a 70/30 M ratio, as described in the Experimental Section. Samples with HF-CNT content of 0.01, 0.1, and 0.3 wt%, as well as a control without CNTs were prepared. These samples were labeled HYD30-CNTY, where Y is the weight percentage of CNT. The different hydrogels were characterized in terms of transparency, mechanical properties, and conductivity at RT; and swelling at different temperatures (to evaluate also thermosensitivity).

Fig. 4a shows the swelling variations as a function of the entire temperature range explored, *i.e.* from 5 to 80 °C for the different hydrogels containing up to 0.3 wt% of HF-CNT. According to our observation, a higher the CNTs loading, leads to a lower swelling, especially at low temperatures, *i.e.* below the VPTT. This behavior can be explained by the hydrophobic contribution of the CNTs. This small hydrophobic contribution also explains the slight decrease of VPTT in the loaded systems from 46 to 42 °C. It is known that hydrophobic contributions shift this transition value towards lower values [48]. In any case, the thermosensitivity can be considered similar because on the one hand, the VPTT variations are rather small (the shapes of the curves are similar), and on the other hand the swelling variations below and above the VPTT are very large in all cases. The wettability analysis using meniscus height has been inserted in Fig. 4a. A slight decrease in the meniscus height can be observed when the CNTs are incorporated into the hydrogel. This observation is in good agreement with the swelling behaviour described in the manuscript.

Regarding the mechanical properties of the hydrogels, which were evaluated at 20 °C in the hydrated state and by compression tests, an evident increase in compression modulus was observed as the HF-CNT content increased, ranging from 0.58 MPa in HYD30 at 20 °C (a value in the range of previously reported VCL-based hydrogels) [7] to 3.7 MPa for HYD30-CNT0.3 samples. This increase in modulus must be related, at least in part, to the reinforcing effect of the load, in agreement with previous literature [49,50]. However, experimental data and predictions described previously for low CNT loads such as those used in this study [51], indicate that the increase is greater than expected. To explain this finding, we can look at the variation in water content, which decreases as the amount of load increases. For hydrogels of the same nature, there is evidence of a relationship between swelling and modulus [7] A reduction in water content similar to that in this study resulted in a modulus 3–4 times higher. Other authors reported similar modulus decrease by plasticization effects [52]. Since the goal in this study is to use these hydrogels for biological applications, it is important to address if cells may be sensitive to these differences in mechanical properties.

This reinforcement effect is in agreement with the study carried out by oscillatory rheology, since stress sweeps (Fig. 4b) confirmed an increase in the hydrogel elastic modulus from 11.2 ± 0.1 MPa for HYD30 to 29.7 ± 2.3 MPa for HYD30-CNT0.3. Furthermore, the width of the linear viscoelastic region (LVR) up to 102 Pa or above was indicative of high stability for all the tested samples, with gel-breaking points (*i.e.* elastic modulus (G') = viscous modulus (G")) occurring at 103 Pa or above. Frequency sweeps (Fig. 4c) confirmed the stability of the hydrogels even at the highest loading level of HF-CNT, with both G' and G'' moduli being independent of the applied frequency across the whole range tested.

The variations in the electrical conductivities of the as-prepared composite hydrogels are quoted in Table 4. HYD30 exhibit $8.6{\cdot}10^{-3} \pm 1.3{\cdot}10^{-3}$ S/m. The increasing HF-CNT content enhances the electrical conductivity by an order of magnitude reaching values from $1.5{\cdot}10^{-2} \pm 3.3{\cdot}10^{-3}$ to $8.1{\cdot}10^{-2} \pm 1.5{\cdot}10^{-2}$ S/m, corresponding to HYD30-CNT0.01

Table 4
Swelling at representative temperatures, VPTT, absorbance, mechanical properties, and conductivity values of the different loaded hydrogels.

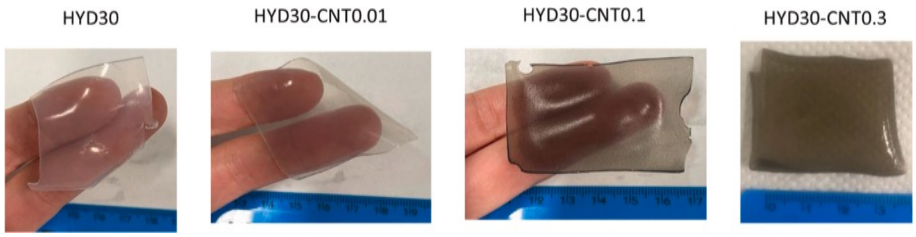

Label	Swelling % at (°C)			VPTT (°C)	Absorbance	Maximum Load (N)	Elongation (%)	Elastic Modulus (MPa)	Conductivity ($S{\cdot}m^{-1}$)
	10	37	60						
HYD30	1590 ± 30	463 ± 25	140 ± 3	46	0.3 ± 0.1	12 ± 1	82 ± 2	0.6 ± 0.2	$8.6{\cdot}10^{-3} \pm 1.3{\cdot}10^{-3}$
HYD30-CNT0.01	1240 ± 70	338 ± 24	118 ± 22	43	0.2 ± 0.0	13 ± 2	72 ± 2	1.7 ± 0.4	$1.5{\cdot}10^{-2} \pm 3.3{\cdot}10^{-3}$
HYD30-CNT0.1	1200 ± 10	300 ± 26	87 ± 17	42	0.6 ± 0.0	13 ± 1	68 ± 1	2.9 ± 0.7	$2.5{\cdot}10^{-2} \pm 1.5{\cdot}10^{-3}$
HYD30-CNT0.3	1070 ± 120	291 ± 48	79 ± 17	42	1.16 ± 0.1	19 ± 2	60 ± 2	3.7 ± 0.5	$8.1{\cdot}10^{-2} \pm 1.5{\cdot}10^{-2}$

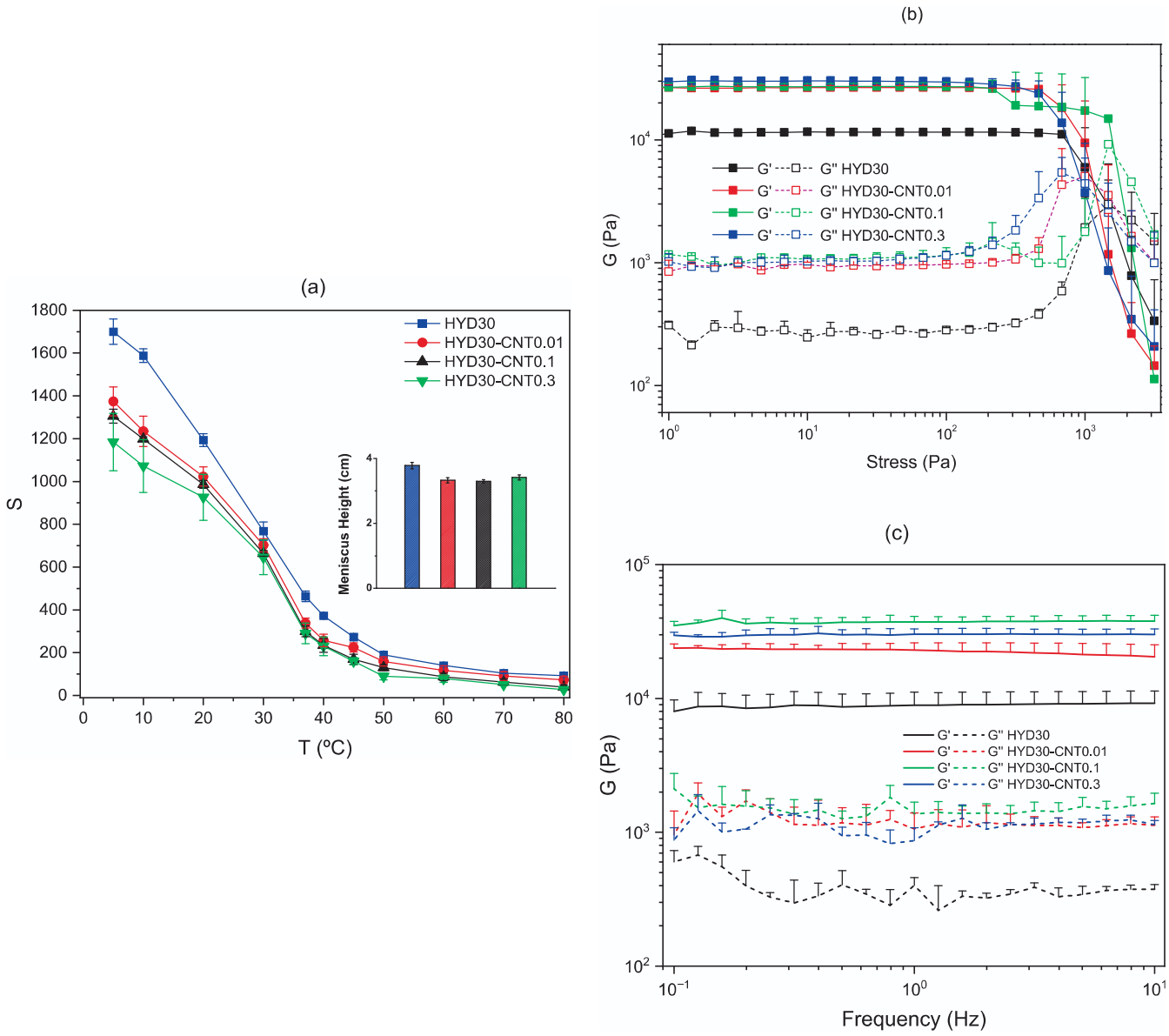

Fig. 4. (a) S, swelling percentage in PBS of the hydrogels prepared using variable amounts of HF-CNT (from 0% or control to 0.3 wt%) as a function of temperature. Right: Oscillatory rheology at room temperature of the loaded hydrogels obtained by photopolymerization. Meniscus height (cm) of the different hydrogels, determined as indicated in Experimental, has been inserted in Fig. 4a. (b) Stress sweeps. (c) Frequency sweeps.

and HYD30-CNT0.3. As a point of interest, electrical conductivity of nerve tissues has been reported in closed ranges, from 10^{-2} to 10^{0} S/m according to some studies [53–57], so that in both cases hydrogels loaded with CNTs are within or very close to the range. Above all, in accord with the results of the compression test, these results manifest the effective enhancement effect of the CNTs on the VCL-based hydrogels in both mechanical and electrical properties.

Improvements in mechanical properties and conductivity must be closely related to the proposed covalent integration of CNTs and their corresponding stable dispersion.

3.2.3. *Biological evaluation of the hydrogels*

3.2.3.1. Biological evaluation of hydrogels with endothelial cultures. Hydrogels with different wt.% of HF-CNT were evaluated as cell harvesting platforms as previously described in section 3.1. Thus, hydrogels were seeded with C166-GFP cells, and micrographs were obtained at 4 h in order to analyze differences in the early adhesion stages. No evidence of a modulation of this mechanism was evidenced (Fig. 5a), with a good response in all platforms. At 48 h, endothelial monolayers were observed proliferating over hydrogels, with high-confluence areas especially in HYD30-CNT0.1 and 0.3.

To validate these observations, double-stranded DNA was quantified in endothelial cultures proliferating over hydrogels. It can be observed in Fig. 5b that the CNTs content upregulated cell growing in these platforms. Especially, CNT0.1 samples reached a high proliferation rate, supporting the micrograph analysis shown before. Thus, we consider that hydrogels containing HF-CNTs did not show any sign of cytotoxicity, and therefore CNTs functionalization maintained hydrogels cytocompatibility.

However, when hydrogels with different % of HF-CNT were used to detach endothelial monolayers by a temperature decrease as previously described, no significant amount of transplanted culture was observed in the new TCP surface. Only a few cells were observed, suggesting that cell attachment to these surfaces is stronger than in control hydrogels, as swelling behaviour was similar.

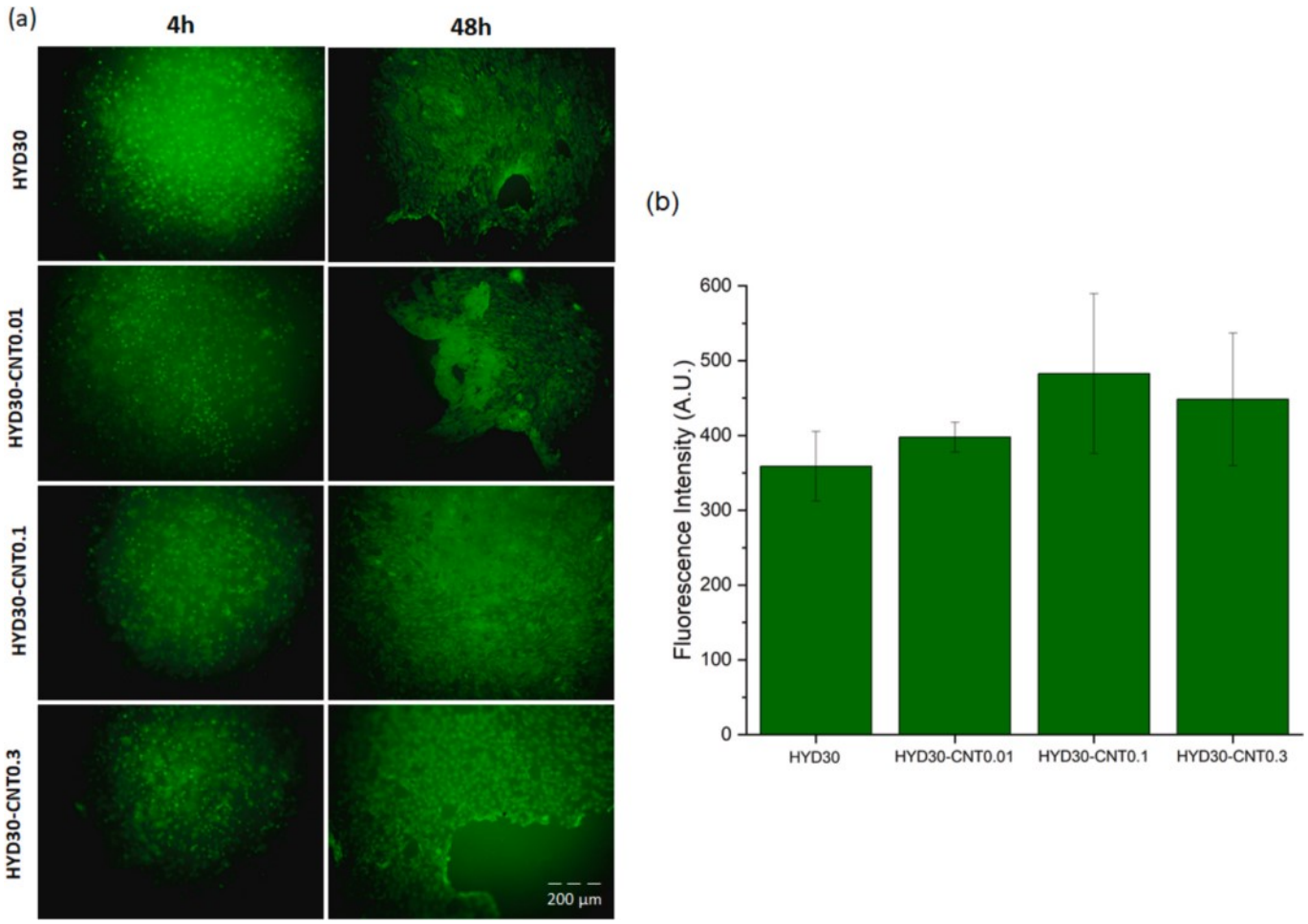

Fig. 5. (a) Fluorescence images of C166-GFP cell cultures on the hydrogels after 4 and 48 h after the seeding process (scale bar: 200 µm). (b) Fluorescence measured (Fluoreporters dsDNA assay) on the different hydrogels after 48 h of the seeding process.

3.2.3.2. Biological evaluation of hydrogels with neuronal cultures. As HF-CNT could affect neuron adhesion, proliferation, and migration, cultures of Neuro2a murine neuroblastoma cell line seeded over hydrogel platforms with 0, 0.01, 0.1, and 0.3 wt% CNT were investigated. Microscopy observation of the cultures revealed that Neuro2a cells grown on all types of hydrogels analyzed, with no differences being observed between platforms. Most of the cells on the hydrogels maintained a spherical shape while, when cultured directly on the plastic bottom of the well, a large part of them took a flattened shape or developed prolongations (Fig. 6). As mentioned before, spherical or round morphology in Neuro2a cells is associated with a loose attachment to the substrate and a high proliferative state, whereas the flattened shape, often associated with the development of non-functional neurites, results from a stronger attachment to the substrate due to the increase in the expression of microtubule-associated proteins and extracellular adhesion proteins [58]. Therefore, it appeared that hydrogels, including CNTs containing hydrogels, limit the flat adherent state of Neuro2a cells in favor of a round proliferative phenotype.

Video time-lapse (VTL) analyses of the numbers of Neuro2a cells in 5 fields per culture on the different hydrogels confirms the proliferative state of Neuro2a when cultured on the hydrogels. As shown in Fig. 6k, the number of cells per field increased a rate comparable to that exhibited on plastic (light blue line) without showing no evident differences associated with the CNT concentration in the hydrogel. In contrast, MTT values (Fig. 6l) suggest that higher concentrations of CNT might slightly increase proliferation, although the effects were clearly non-significant. Thus, although hydrogels promoted a proliferative, round-shaped morphology of Neuro2a cells compared with cultures on plastic, this did not translate into an overall increase in proliferation. Considering that Neuro2a cells are widely used as a platform for neurotoxicity studies —allowing evaluation of the effects of drugs, environmental toxins, and other chemical agents on neuronal survival [59]— the comparable proliferation observed on plastic and on HF-CNT hydrogels suggests that these hydrogels do not exert marked neurotoxic effects. However, additional analyses involving primary cultures of neural cells will be required to confirm the lack of neurotoxicity with higher confidence.

A final aspect revealed by the VTL analyses of the cultures over hydrogels was the lack of cell migration. While Neuro2a showed a great capacity for movement when seeded directly on plastic plates, when cultured on hydrogels hardly any cell movement was observed. Therefore, the hydrogels, irrespectively of the CNT loading, promote a proliferative, round-shaped, and non-migrating Neuro2a phenotype. These observations indicate that there is no influence of CNT loading on cell response. Nevertheless, these studies are preliminary and, given the contribution of CNTs to conductivity, should be further confirmed and amplified.

4. Conclusions

This study has demonstrated the successful optimization of hydrogels based on thermosensitive poly-(VCL-co-VP) copolymers with tailored variations in the VPTT, resulting in modulated performance characteristics of the hydrogel systems such as more swelling at room

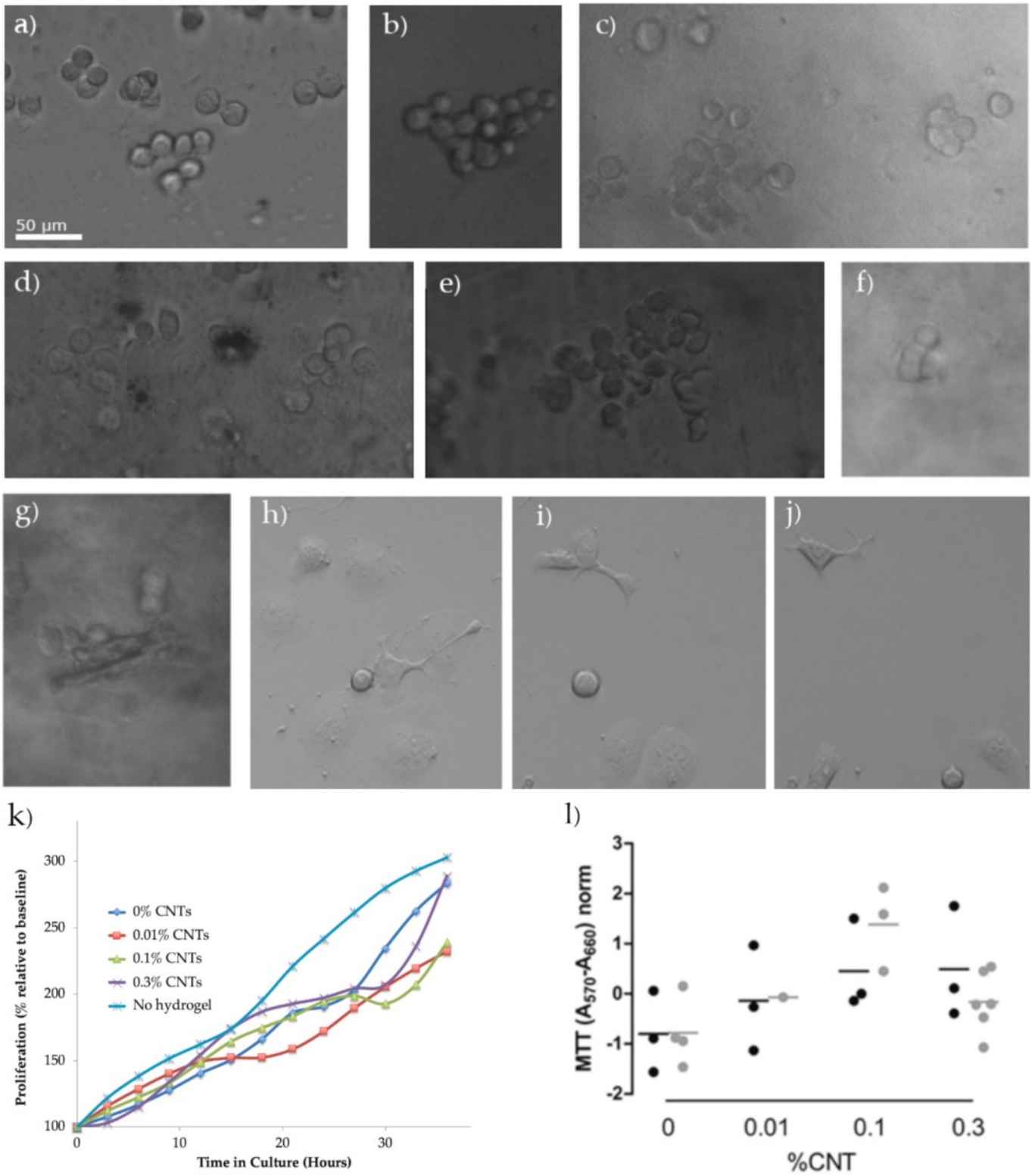

Fig. 6. Neuro2a cultures on hydrogels. a-j) Representative images of Neuro2a cells cultured on different hydrogels or on plastic (control) showing the absence of flattened-shaped cells when cultured on the hydrogels. a) HYD30 after 12 h. b) and c) HYD30-CNT0.01 after 42 and 48 h, respectively. d) and e) HYD30-CNT0.1 after 36 and 48 h. f) and g) HYD30-CNT0.3 after 24 and 27 h. h), i) and j) Cultures on plastic 48, 24, and 0 h after seeding. Except for control images that were obtained from the same field, all others correspond to different wells or fields. Scale bar in (a) applies to all images. k) Proliferation on the different hydrogels, expressed as the number of cells per field every 3 h (over 36 h). Values are expressed as a percentage relative to seeding time. l) MTT values after 48 h of culture on the hydrogels. Values were standardized to allow comparison between two independent experiments.

temperature. The functionalization of CNTs was effectively achieved, enabling their homogeneous impregnation into the copolymer matrix, leading to good dispersion in the matrix until 0.3 wt%. The incorporation of high-functionalization CNTs significantly improved the mechanical and conductive properties of the hydrogels. Importantly, adhesion and proliferation in C-166 endothelial cell line were positively correlated with the increasing percentage of HF-CNT in the hydrogel composition, indicating their potential in supporting cellular activities. Furthermore, the hydrogels were compatible with alternative cell lines, including Neuro2a neuronal cell line, showing promising results in terms of cellular integration and functionality. These findings collectively highlight the potential of VCL-VP copolymer-based hydrogels, reinforced with functionalized CNTs, as robust platforms for a wide range of biomedical applications, including tissue engineering and regenerative medicine.

CRediT authorship contribution statement

Pedro Liz-Basteiro: Writing – original draft, Validation, Methodology, Investigation, Formal analysis. **Goretti Arias-Ferreiro:** Writing – review & editing, Writing – original draft, Validation, Investigation, Formal analysis. **Davide Marin:** Writing – original draft, Validation, Methodology, Formal analysis, Data curation. **Enrique Martínez-Campos:** Writing – original draft, Validation, Methodology, Investigation, Data curation. **Helmut Reinecke:** Writing – original draft, Validation, Resources, Data curation. **Carlos Elvira:** Writing – original draft, Methodology, Investigation, Formal analysis, Conceptualization. **Juan Rodríguez-Hernandez:** Writing – original draft, Validation, Methodology, Funding acquisition, Data curation, Conceptualization. **Manuel Nieto-Diaz:** Writing – original draft, Validation, Investigation, Data curation, Conceptualization. **David Reigada:** Writing – review & editing, Methodology, Investigation, Formal analysis, Conceptualization. **Rodrigo M. Maza:** Writing – review & editing, Validation, Investigation, Formal analysis, Data curation. **Silvia Marchesan:** Writing – original draft, Validation, Methodology, Investigation, Data curation, Conceptualization. **Alberto Gallardo:** Supervision, Project administration, Methodology, Formal analysis, Data curation.

Declaration of competing interest

The authors declare the following financial interests/personal relationships which may be considered as potential competing interests: Alberto Gallardo reports financial support was provided by Spain Ministry of Science and Innovation. If there are other authors, they declare that they have no known competing financial interests or personal relationships that could have appeared to influence the work reported in this paper.

Acknowledgements

Consejo Superior de Investigaciones Científicas. Project PDC2022-133446-I00 funded by MICIU/AEI /10.13039/501100011033, Spain, and by European Union Next GenerationEU/ PRTR. Project PID2023-151687OB-I00 funded by MICIU/AEI/10.13039/501100011033, Spain, and by FEDER, UE.

Data availability

Data will be made available on request.

References

[1] X. Li, et al., A PNIPAAm-based thermosensitive hydrogel containing SWCNTs for stem cell transplantation in myocardial repair, Biomaterials 35 (2014) 5679–5688.
[2] I. Strokov, S. Abramchuk, E. Makhaeva, Salt and pH effect on thermoresponsive behavior of multiwalled carbon nanotube (MWCNT)/poly(N-vinylcaprolactam) dispersion, Colloid Polym. Sci. 297 (2019).
[3] M.F.L. De Volder, S.H. Tawfick, R.H. Baughman, A.J. Hart, Carbon nanotubes: present and future commercial applications, Science 1979 (339) (2013) 535–539.
[4] D. Tasis, N. Tagmatarchis, A. Bianco, M. Prato, Chemistry of carbon nanotubes, Chem. Rev. 106 (2006) 1105–1136.
[5] N.G. Sahoo, S. Rana, J.W. Cho, L. Li, S.H. Chan, Polymer nanocomposites based on functionalized carbon nanotubes, Prog. Polym. Sci. 35 (2010) 837–867.
[6] S. Shin, et al., Carbon-nanotube-embedded hydrogel sheets for engineering cardiac constructs and bioactuators, ACS Nano 7 (2013).
[7] R. García-Sobrino, et al., Cell harvesting on robust smart thermosensitive pseudo-double networks prepared by one-step procedure, Eur. Polym. J. 209 (2024) 112925.
[8] R. García-Sobrino, et al., Fabrication of 3D cylindrical thermosensitive hydrogels as supports for cell culture and detachment of tubular cell sheets, Biomater. Adv. 144 (2022) 213210.
[9] R. García-Sobrino, et al., Hydrogels with dual sensitivity to temperature and pH in physiologically relevant ranges as supports for versatile controlled cell detachment, Biomater. Adv. 159 (2024) 213826.
[10] E. Martínez-Campos, et al., Thermosensitive hydrogel platforms with modulated ionic load for optimal cell sheet harvesting, Eur. Polym. J. 103 (2018).
[11] Z. Liu, A. Lu, Z. Yang, Y. Luo, Enhanced swelling and mechanical properties of P (AM-co-SMA) semi-IPN composite hydrogels by impregnation with PANI and MWNTs-COOH, Macromol. Res. 21 (2013) 376–384.
[12] R.A. MacDonald, C.M. Voge, M. Kariolis, J.P. Stegemann, Carbon nanotubes increase the electrical conductivity of fibroblast-seeded collagen hydrogels, Acta Biomater. 4 (2008) 1583–1592.
[13] K. Sui, S. Gao, W. Wu, Y. Xia, Injectable supramolecular hybrid hydrogels formed by MWNT-grafted-poly(ethylene glycol) and α-cyclodextrin, J. Polym. Sci. A Polym. Chem. 48 (2010) 3145–3151.
[14] S.R. Shin, et al., Aligned carbon nanotube–based flexible gel substrates for engineering biohybrid tissue actuators, Adv. Funct. Mater. 25 (2015) 4486–4495.
[15] A. Adewunmi, S. Ismail, A. Sultan, Carbon nanotubes (CNTs) nanocomposite hydrogels developed for various applications: a critical review, J. Inorg. Organomet. Polym Mater. 26 (2016).
[16] H. Ravanbakhsh, G. Bao, L. Mongeau, Carbon nanotubes promote cell migration in hydrogels, Sci. Rep. 10 (2020) 2543.
[17] X. Liu, et al., 3D-printed scaffolds with carbon nanotubes for bone tissue engineering: fast and homogeneous one-step functionalization, Acta Biomater. 111 (2020) 129–140.
[18] J. Zhang, A. Wang, pH- and thermo-responsive dispersion of single-walled carbon nanotubes modified with poly(N-isopropylacrylamide-co-acrylic acid), J. Colloid Interface Sci. 334 (2009) 212–216.
[19] S. Soll, M. Antonietti, J. Yuan, Double stimuli-responsive copolymer stabilizers for multiwalled carbon nanotubes, ACS Macro Lett. 1 (1) (2012) 84–87.
[20] Z. Li, M. Tang, W. Bai, R. Bai, Preparation of hydrophilic encapsulated carbon nanotubes with polymer brushes and its application in composite hydrogels, Langmuir 33 (2017).
[21] A.A. Alencar de Queiroz, A. Gallardo, J. San Román, Vinylpyrrolidone–N, N′-dimethylacrylamide water-soluble copolymers: synthesis, physical–chemical properties and proteic interactions, Biomaterials 21 (2000) 1631–1643.
[22] I. Aranaz, H. Reinecke, C. Elvira, A. Gallardo, Compositionally-tunable surface nanostructuration of microspheres obtained from a self-stabilizing copolymerization of methylmethacrylate and vinylpyrrolidone, Poly. (Guildf) 52 (2011) 2991–2997.
[23] M. Guvendiren, M. Perepelyuk, R.G. Wells, J.A. Burdick, Hydrogels with differential and patterned mechanics to study stiffness-mediated myofibroblastic differentiation of hepatic stellate cells, J. Mech. Behav. Biomed. Mater. 38 (2014) 198–208.
[24] C. Gao, S. Song, Y. Lv, J. Huang, Z. Zhang, Recent development of conductive hydrogels for tissue engineering: review and perspective, Macromol. Biosci. 22 (2022) 2200051.
[25] C. Qin, et al., Advances in conductive hydrogel for spinal cord injury repair and regeneration, Int. J. Nanomedicine 18 (2023) 7305–7333.
[26] I. Aranaz, et al., Pseudo-double network hydrogels with unique properties as supports for cell manipulation, J. Mater. Chem. B 2 (2014) 3839–3848.
[27] D.Y. Kwok, C.J. Budziak, A.W. Neumann, Measurements of static and low rate dynamic contact angles by means of an automated capillary rise technique, J. Colloid Interface Sci. 173 (1995) 143–150.
[28] Yuan, Y. & Lee, T. R. Contact Angle and Wetting Properties. in *Surface Science Techniques* (eds. Bracco, G. & Holst, B.) 3–34 (Springer Berlin Heidelberg, Berlin, Heidelberg, 2013). doi:10.1007/978-3-642-34243-1_1.
[29] D. Zehm, A. Lieske, A. Stoll, On the thermoresponsivity and scalability of N,N-dimethylacrylamide modified NIPAM microgels, Macromol. Chem. Phys. 221 (2020) 2000018.
[30] K. Kolewe, S. Peyton, J. Schiffman, Fewer bacteria adhere to softer hydrogels, ACS Appl. Mater. Interfaces 7 (2015).
[31] P. Costa, et al., Effect of carbon nanotube type and functionalization on the electrical, thermal, mechanical and electromechanical properties of carbon nanotube/styrene–butadiene–styrene composites for large strain sensor applications, Compos. B Eng. 61 (2014) 136–146.
[32] H. Lorenz, et al., Advanced elastomer nano-composites based on CNT-hybrid filler systems, Compos. Sci. Technol. 69 (2009) 2135–2143.
[33] A. Das, et al., Modified and unmodified multiwalled carbon nanotubes in high performance solution-styrene-butadiene and butadiene rubber blends, Poly. (Guildf) 49 (2008) 5276–5283.
[34] J.L. Bahr, J.M. Tour, Covalent chemistry of single-wall carbon nanotubes, J. Mater. Chem. 12 (2002) 1952–1958.

[35] B.K. Price, J.M. Tour, Functionalization of single-walled carbon nanotubes "on water", J. Am. Chem. Soc. 128 (2006) 12899–12904.
[36] J. Bahr, J. Tour, Highly functionalized carbon nanotubes using in situ generated diazonium compounds, Chem. Mater. - CHEM MATER 13 (2001).
[37] C. Dyke, J. Tour, Solvent-free functionalization of carbon nanotubes, J. Am. Chem. Soc. 125 (2003) 1156–1157.
[38] S. Marchesan, K. Kostarelos, A. Bianco, M. Prato, The winding road for carbon nanotubes in nanomedicine, Mater. Today 18 (2015) 12–19.
[39] S. Bosi, et al., Carbon based substrates for interfacing neurons: comparing pristine with functionalized carbon nanotubes effects on cultured neuronal networks, Carbon N Y 97 (2016) 87–91.
[40] A. Tomova, et al., Functionalization and characterization of MWCNT produced by different methods, Acta Phys. Pol. A 129 (2016) 405–408.
[41] S. Costa, E. Borowiak-Palen, M. Kruszynska, A. Bachmatiuk, R. Kalenczuk, Characterization of carbon nanotubes by Raman spectroscopy, Mater. Sci.- Poland 26 (2008).
[42] R.R. Nayak, K.Y. Lee, A.M. Shanmugharaj, S.H. Ryu, Synthesis and characterization of styrene grafted carbon nanotube and its polystyrene nanocomposite, Eur. Polym. J. 43 (2007) 4916–4923.
[43] R. Tian, et al., An efficient route to functionalize singe-walled carbon nanotubes using alcohols, Appl. Surf. Sci. 255 (2008) 3294–3299.
[44] L.K. Noda, O. Sala, A resonance Raman investigation on the interaction of styrene and 4-methyl styrene oligomers on sulphated titanium oxide, Spectrochim. Acta A Mol. Biomol. Spectrosc. 56 (2000) 145–155.
[45] P. Rozhin, et al., Nanocomposite hydrogels with self-assembling peptide-functionalized carbon nanostructures, Chem. – A Eur. J. 29 (2023) e202301708.
[46] S. Marchesan, M. Melchionna, M. Prato, Wire up on carbon nanostructures! how to play a winning game, ACS Nano 9 (2015) 9441–9450.
[47] W. Deng, et al., A tough, stretchable, adhesive and electroconductive polyacrylamide hydrogel sensor incorporated with sulfonated nanocellulose and carbon nanotubes, Int. J. Biol. Macromol. 279 (2024) 135165.
[48] M.R. Aguilar, C. Elvira, A. Gallardo, B. Vazquez, J. Román, Smart polymers and their applications as biomaterials, Top. Tissue Eng. 3 (2007).
[49] A. Bratovcic, Nanocomposite hydrogels reinforced by carbon nanotubes, Int. J. Eng. Res. Appl. 10 (2020) 30–41.
[50] P. Rozhin, S. Kralj, B. Soula, S. Marchesan, E. Flahaut, Hydrogels from a self-assembling tripeptide and carbon nanotubes (CNTs): comparison between single-walled and double-walled CNTs, Nanomaterials 13 (2023).
[51] J. Reif, et al., Enhanced mechanical properties of nanocomposites at low graphene content, ACS Nano 3 (2009) 3884–3890.
[52] Q. Zheng, et al., In-situ polymerization of pyrrole on cellulose nanofiber film: structure characterization and electrochemical properties, Ind. Crops Prod. 222 (2024) 120068.
[53] X. Liu, et al., Functionalized carbon nanotube and graphene oxide embedded electric conductive hydrogel synergistically stimulates nerve cell differentiation, ACS Appl. Mater. Interfaces 9 (2017).
[54] Roth, B. The Electrical Conductivity of Tissues. in (2000).
[55] J.B. Ranck, S.L. BeMent, The specific impedance of the dorsal columns of cat: an anisotropic medium, Exp. Neurol. 11 (1965) 451–463.
[56] I. Tasaki, A new measurement of action currents developed by single nodes of Ranvier, J. Neurophysiol. 27 (1964) 1199–1206.
[57] H. McCann, G. Pisano, L. Beltrachini, Variation in reported human head tissue electrical conductivity values, Brain Topogr. 32 (2019).
[58] Tremblay, R. *et al.* Differentiation of N2a cells into dopamine neurons. (2008).
[59] K. LePage, R. Dickey, W. Gerwick, E. Jester, T. Murray, On the use of neuro-2a neuroblastoma cells versus intact neurons in primary culture for neurotoxicity studies, Crit. Rev. Neurobiol. 17 (2005) 27–50.